

# EUROPEAN ORGANIZATION FOR NUCLEAR RESEARCH

## Letter of Intent to the ISOLDE and Neutron Time-of-Flight Committee

### Development of vanadium beams at ISOLDE

September 26, 2023

B. Olaizola<sup>1</sup>, A. Algora<sup>2</sup>, Y. Ayyad<sup>3</sup>, M. J. G. Borge<sup>1</sup>, J. A. Briz<sup>4</sup>, J. Cubiss<sup>5</sup>,  
B. Errandonea-Felix<sup>1</sup>, L. M. Fraile<sup>4</sup>, A. Illana<sup>4</sup>, U. Koester<sup>6</sup>, R. Lică<sup>7</sup>, C. Mihai<sup>7</sup>,  
J. Sanchez-Prieto<sup>1</sup>, K. Wimmer<sup>8</sup>

<sup>1</sup>*IEM-CSIC, Madrid, Spain*

<sup>2</sup>*IFIC Valencia, Spain*

<sup>3</sup>*Universidad de Santiago, Spain*

<sup>4</sup>*Universidad Complutense de Madrid, Spain*

<sup>5</sup>*University of York, UK*

<sup>6</sup>*ILL Grenoble, France*

<sup>7</sup>*IFIN-HH Bucharest, Romania*

<sup>8</sup>*GSI Darmstadt, Germany*

**Spokesperson:** [B. Olaizola] [bruno.olaizola@csic.es]

**Contact person:** [M. Au] [mia.au@cern.ch], [K. Chrysalidis]  
[katerina.chrysalidis@cern.ch]

**Abstract:** This letter of intent proposes the development of intense and pure V beams in order to study their decay into Cr isotopes and unravel their nuclear structure when approaching  $N = 40$ . The future experiment aims to systematically measure  $\tau(2_1^+)$  and locate  $0^+$  states in the even-A isotopes to establish shape coexistence in this Island of Inversion. The odd-A isotopes will be studied to extract single particle energies and intruder states. Due to the refractory character of V and the short half-lives of neutron-rich V isotopes, beam development is requested to identify the most promising approach towards delivery of the isotopes of interest.

**Requested shifts:** 6 shifts, (split into 2 runs over 1 year)

**Installation:** [IDS and/or Fast Tape Station, if required]



# 1 Scientific value

One of the more well-known divergences from a naive independent-particle shell model description of the nucleus is the existence of islands of inversion [1]. Several islands of inversion have been suggested throughout the nuclear chart, at  $N = 8, 14, 28, 40$ , and, recently suggested, 50 [2, 3, 4, 5, 6]. In these islands, the ground-state configurations of even-even nuclei are dominated by particle-hole ( $np - nh$ ) intruder configurations rather than the  $0p0h$  configurations predicted by spherical mean-field calculations at stability [1]. As a consequence, the features normally observed in regions located near a large shell or sub-shell closure disappear: a smooth evolution of the  $2_1^+$  energies and  $B(E2; 2_1^+ \rightarrow 0_1^+)$  values, with no sudden increases or decreases, respectively (as seen, for example, in Fig 1 for the Ni chain at  $N = 40$ ). These regions can also be identified experimentally by tracking yrast states of odd nuclei and observing an inversion of the expected order [7].

Recent experimental and theoretical developments have focused on the  $N = 40$  island of inversion [8]. Though not a traditional “magic number”,  $N = 40$  represent the boundary between the negative-parity  $pf$  shell and the positive-parity  $0g_{9/2}$  and  $1d_{5/2}$  shell. In stable nuclei, the  $g_{9/2}$  orbital is close enough to the  $pf$  shell to reduce this shell gap resulting in a stable sub-shell closure at  $N = 50$ . Measurements of  $B(E2)$  values and  $E(2_1^+)$  in the region show increased collectivity through the  $N = 40$  shell gap, with the clear exception of  $^{68}\text{Ni}$  (Fig. 1). Deformation and shape co-existence have been identified in the area [9, 10, 11, 12] and a combination of calculation and experimental results suggest an inversion of levels [8]. The inversion of the levels seen for the  $N \approx 40$  nuclides below the valley of stability is attributed to the weakening of the proton-neutron tensor interaction as protons are removed from the  $\pi 0f_{7/2}$  orbital, resulting in a repulsion of the  $\nu 0f_{5/2}$  and attraction of the  $\nu 0g_{9/2}$  orbitals [13]. The LNPS shell-model interaction [8] has had significant success describing nuclei in this region [9, 14, 11, 15]. This interaction includes the full  $pf$  shell for protons and the  $0f_{5/2}, 1p_{3/2}, 1p_{1/2}, 0g_{9/2}$ , and  $1d_{5/2}$  orbitals for neutrons. The evolution of the Ni isotopic chain has been described in terms of the so called *Type 2 Shell Evolution* [16]. Using Monte Carlo shell model calculations in a large valence space, the authors predict the coexistence of spherical ground states with strongly-deformed  $0^+$  states at low energies.

Recent measurements at RIKEN suggest that this island of inversion extends beyond  $N = 40$  toward the magic  $N = 50$  [17], which has been later supported by large scale shell model calculations [5]. Such an extension has precedent in the proposed merging of the islands of inversion at  $N = 20$  and  $N = 28$  [18]. The systematics of the magnesium, neon, and silicon isotopes all suggest an area of continuous collectivity. Though only a few experiments have been able to directly measure  $^{40}\text{Mg}_{28}$ , which lies close to the neutron drip-line, they suggest that the deformation of the Mg isotopes continues to  $N = 28$  [19]. Large-scale shell model calculations that reproduce the excitation energies and  $B(E2)$  values in the region also predict a steadily increasing occupancy of the  $\nu p_{3/2}$  orbital with increasing mass in the  $^{30-42}\text{Mg}$  isotopic chain [15].

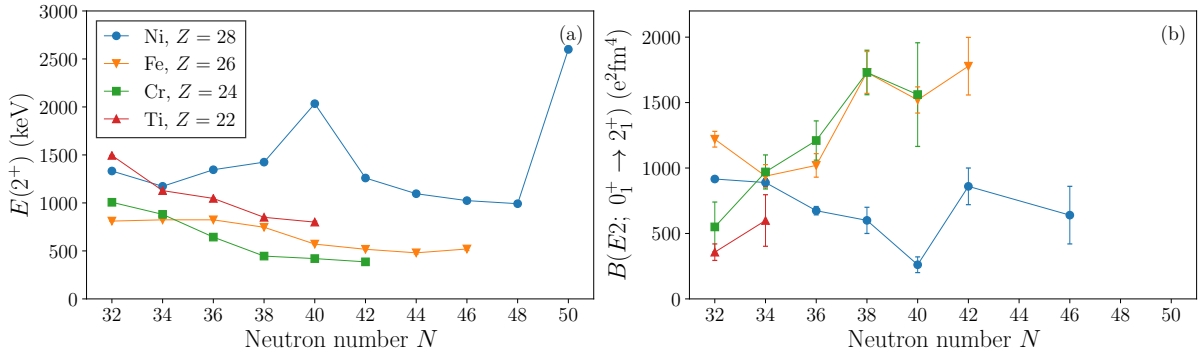


Figure 1: (a) Systematics of the  $2_1^+$  states near  $^{68}\text{Ni}^{40}$ . (b)  $B(E2; 0_1^+ \rightarrow 2_1^+)$  values for the same region of the nuclear chart. Figure adapted from Ref. [20].

### 1.1 Direct measurement of $^{64}\text{Cr}$ $\tau(2_1^+)$

All models predict the center and maximum of collectivity for this island of inversion at  $^{64}\text{Cr}$  ( $N = 40$ ) [8, 21]. Despite the agreement among theoretical calculations,  $^{62}\text{Cr}$  and  $^{64}\text{Fe}$  (both  $N = 38$ ) possess larger  $B(E2)$  than  $^{64}\text{Cr}$ , as can be seen in the right panel of Fig. 1. Even when translated to deformation as expressed by the  $\beta_2$  parameter,  $^{62}\text{Cr}$  still presents a larger value than  $^{64}\text{Cr}$ . Even more so, the Fe isotope chain suggests a local minimum at  $N = 40$ , with the  $\beta_2$  value of  $^{64}\text{Fe}$  being more than one  $\sigma$  larger than that of  $^{66}\text{Fe}$ . These discrepancies with theoretical predictions could be explained by the significant error bars, specially that of the  $B(E2)$  of  $^{64}\text{Cr}$ , which currently is larger than 25%. This  $N = 40$  island of inversion is often compared to the  $N = 20$  one due to its similarities. However, if a significantly larger deformation at  $N = 38$  than at 40 is confirmed, this would point to a remarkable difference with the lighter island of inversion, where deformation smoothly increases as we move towards its center. No set of calculations has been able to reproduce this irregular trend at  $N = 40$  [22]. This situation of the experimental values, in clear contrast to theoretical models, calls for new and independent measurement of these  $B(E2)$  values to clarify the evolution of collectivity in the region.

### 1.2 Intruder states in $^{63}\text{Cr}$

The study of  $N = 39$  isotones gives access to intruder states. In a previous study of the  $^{65}\text{Mn}$  decay at ISOLDE [14] the nature of normal negative parity  $fp$  states and intruder states originating from the promotion of particles to the positive parity  $0g_{9/2}$  and  $1d_{5/2}$  orbitals. The latter two are isomeric, demonstrating their single-particle nature. In the next even- $Z$  isotone  $^{63}\text{Cr}$ , only three  $\gamma$  rays and two excited states have been identified [23]. In our previous experiment RIBF140 we searched for isomeric states in  $^{63}\text{Cr}$  however no long lived state was identified [24]. LNPS calculations [8, 22] associate  $J^\pi = 3/2^-, 5/2^-,$  and  $1/2^-$  with the ground and first two excited states. The excitation energies are in good agreement with the proposed cascade decay [23]. The calculations predict two positive parity states at around 500 keV. We propose to identify these positive parity states and therefore complete the systematics of  $9/2^+$  states in  $N = 39$  isotopes. Based on the known data for Fe and Ti [14, 24] and the LNPS predictions [22] we expect

that the energies of the positive parity states reach a minimum at  $Z = 24$ . This is where the maximum of collectivity as function of  $Z$  results in the lowest  $E(2^+)$  in the even-even nuclei. The maximum of particle-hole correlations is expected to also yield large transition strengths for the decay of states in the  $N = 39$  isotopes. Excited state lifetime measurements will thus yield the experimental signatures of intruder states in  $^{63}\text{Cr}$ .

## 2 Planned experiments

Since V beams have never been extracted at ISOLDE, there is a wide range of possible experiments that could be performed, such as mass measurements, transfer reactions or laser spectroscopy. For the sake of this LoI, we will focus on V decay experiments to study Cr isotopes at IDS.

The ultimate goal of this LoI is to produce  $^{64}\text{V}$  with enough intensity, a challenging feat. IDS has shown that it is able to extract nuclear structure information with beam intensities as low as 2 ions/ $\mu\text{C}$  (see, for example, Ref. [25]). The significant upgrade planned for IDS (from 4 HPGe clovers to up to 15, for instance) guarantees that it will be able to perform experiments with even weaker beams.

Example of planned experiments:

### 2.1 Search for $0^+$ states

Thanks to the aforementioned upgrade, IDS will be able to perform  $\gamma - \gamma$  angular correlations with enough precision to determine the multiplicities of transitions, and the spins and parities of connected states. Specifically,  $0 \rightarrow 2 \rightarrow 0$  cascades are some of the most anisotropic ones, which allows to firmly establish the  $0^+$  character of a state with as low as 5-10k coincidences. Additionally, the SPEDE detector can be used to measure E0 transitions, another powerful tool to locate  $0^+$  states, among other things.

For the neutron-rich Cr isotopic chain, excited  $0^+$  states have only been firmly established for  $^{54}\text{Cr}$ , a stable isotope. Above it, only for  $^{56}\text{Cr}$  a tentative  $0^+$  state has been suggested at 1.67 MeV. This state is strongly populated in the  $\beta$  decay of  $^{56}\text{V}$ , so it should be easy to perform angular correlations. As we move towards the IoI, we can expect these  $0^+$  states to remain low in energy or even drop. The spherical shell model predicts that V isotopes in this region to have  $J^\pi = 1^+$ . If this is the case, we can expect the Cr  $0^+$  excited states to be significantly populated in  $\beta$  decay.

Complementary to angular correlations,  $0^+$  states can be firmly established by directly measuring their E0 transitions. This conversion electrons can be detected using the Si array SPEDE. The combination of simultaneously measuring angular correlations and conversion electrons also allows to extract the E0 component of  $J \rightarrow J$  transitions. The presence of strong E0 components is a clear indication of shape coexistence [26].

It should be noted that the  $\beta$  decay of even-A V isotopes is poorly studied, with only a handful of events detected so far. For instance, for the decay of  $^{58}\text{V}$  (g.s.  $(1^+)$ ), it is suggested that it mainly populates  $4^+$  states in  $^{58}\text{Cr}$ , which is physically impossible. This is just an example of how incomplete the Cr level scheme are known.

## 2.2 Fast-timing experiments

The  $N = 40$  island of inversion is characterized by the promotion of neutrons from the negative-parity  $pf$  shell into the positive-parity  $g_{9/2}$  and  $d_{5/2}$  orbitals. For the odd-A even- $Z$  nuclei, this change of parity causes the appearance of long-lived isomers, generally with  $J^\pi = 9/2^+$  (for the Fe chain, see Refs. [27, 14, 28]). For the case of Cr isotopes, this isomeric state is only firmly established for  $^{55}\text{Cr}$  and its lifetime is only measured for  $^{59}\text{Cr}$ . Completing the systematics of this isomer into the island of inversion would give information on the single particle states evolution.

As it is common, these odd-A Cr isotopes all present several low-energy transitions, for which the parent levels can be expected to have lifetimes in the nano to picosecond range. This time range is accessible for the  $\text{LaBr}_3(\text{Ce})$  IDS scintillators, which can perform precision fast-timing measurements to extract their lifetimes. These lifetimes are the, generally, most difficult ingredient to obtain when trying to extract transition strengths  $[\text{B}(\text{XL})]$ , which are one of the most stringent tests available for shell model calculations. Lifetimes have only been measured for the stable  $^{53}\text{Cr}$  and a couple of values for  $^{55}\text{Cr}$ . Above it, no excited level lifetime has been measured.

Additionally, as it was discussed in Sec. 1.1, a direct measurement of the  $\tau(2_1^+)$  value of the even-A Cr would help to clarify the evolution of deformation for the  $N = 40$  island of inversion.

## 2.3 Beamtime estimations

Since the level schemes of neutron-rich Cr isotopes are poorly known, especially when populated in the  $\beta$  decay of V, the beamtime estimations presented are highly speculative. As an example, the most ambitious measurement of the  $\tau(2_1^+)$  for  $^{64}\text{Cr}$  will be employed:

The  $B(E2; 2_1^+ \rightarrow 0_1^+)$  value was measured in a Coulomb excitation experiment, for which  $T_{1/2} = 125(50)$  ps was extracted, supporting the enhanced collectivity of this nucleus [9]. Tentative  $(4^+)$  and  $(6^+)$  states have been proposed in a recent in-beam  $\gamma$ -spectroscopy experiment [29]. There has only been one previous  $\beta$ -decay experiment, which barely observed 3-4 counts in the  $2_1^+ \rightarrow 0_1^+$  transition [23], see Fig. 2. Due to the limited statistics, the authors stated that they could not rule out that the population of the  $2_1^+$  proceeded entirely via other states, such as the  $4_1^+$ . None of the known levels are a candidate for a  $0_2^+$  state.

Assuming a beam intensity of  $\sim 1$  pps at IDS for  $^{64}\text{V}$ , we should expect over  $4.3 \cdot 10^5$  decays in 5 days of beam-time, at least a factor of 3000 more statistics than the previous decay experiment [23]. This will allow constructing the level scheme using  $\gamma - \gamma$  coincidences, and locating a candidate for the  $0_2^+$  state, predicted at  $\sim 1.6$  MeV by the LNPS interaction [29]. The g.s.  $J^\pi$  in  $^{64}\text{V}$  is unknown, but theoretical calculations predict that it originates from the coupling of  $\Omega_p = 5/2^-$  and  $\Omega_n = 9/2^+$ , therefore we can expect  $2 - 7^-$ . Given that range, we will assume that the  $2_1^+$  state is populated by a  $\gamma$  transition from above with a total intensity of  $\sim 30\%$  (the  $4_1^+ \rightarrow 2_1^+$ , for example).

Assuming  $4.3 \cdot 10^5$  decays, 40%  $\beta$  efficiency, 6% and 10%  $\gamma$  efficiency and 30% absolute intensity, around 300  $\beta - \gamma - \gamma$  coincidences can be recorded in 5 days beamtime, enough

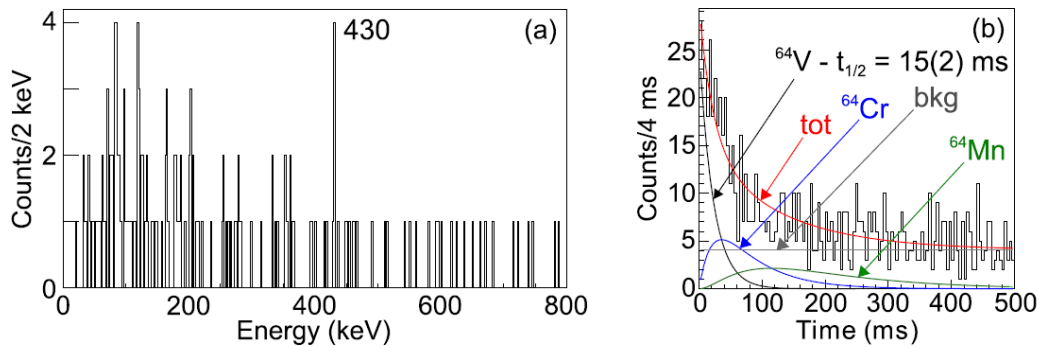


Figure 2: (a) The  $\gamma$ -ray spectrum following the decay of  $^{64}\text{V}$ . (b) The  $\beta$ -decay curve used to extract the  $^{64}\text{V}$  lifetime. Figure adapted from Ref. [23].

to measure the half-life down to a  $\sim 15\%$  precision.

### 3 Beam development

The short half-life and refractory chemical properties of vanadium present a challenge for ion beam production. Molecular beams have been used as an approach to improve extraction rates of other refractory species such as boron [30] and to reduce isobaric contamination [31]. Extraction of vanadium isotopes in the form of volatile molecules (e.g.  $\text{VF}_x$ ) may offer improved efficiencies, but further studies are required to determine the applicability of the method to  $^{64}\text{V}$ , with a half-life of 15 ms. Alternative approaches involve the development of high-efficiency resonance laser ionization schemes used in combination with new target and ion source designs. An offline experimental campaign for the comparison of the two production methods prior to online production tests could provide initial identification of the most promising approach to deliver this challenging beam, which can then be pursued in an online yield measurement campaign.

Both, the RILIS and TISD groups have expressed their interest in developing V beams. Personnel has already been assigned (*i.e.* the contact people) for their development.

**Summary of requested shifts:** 6 shifts split into 2 runs.

## References

- [1] B. A. Brown. Islands of insight in the nuclear chart. *Physics*, 3:104, dec 2010.
- [2] B. Bastin, S. Grévy, D. Sohler, O. Sorlin, Zs. Dombrádi, N. L. Achouri, J. C. Angélique, F. Azaiez, D. Baiborodin, R. Borcea, C. Bourgeois, A. Buta, A. Bürger, R. Chapman, J. C. Dalouzy, Z. Dlouhy, A. Drouard, Z. Elekes, S. Franchoo, S. Iacob,

- B. Laurent, M. Lazar, X. Liang, E. Liénard, J. Mrazek, L. Nalpas, F. Negoita, N. A. Orr, Y. Penionzhkevich, Zs. Podolyák, F. Pougheon, P. Roussel-Chomaz, M. G. Saint-Laurent, M. Stanoiu, I. Stefan, F. Nowacki, and A. Poves. Collapse of the  $n = 28$  shell closure in  $^{42}\text{Si}$ . *Phys. Rev. Lett.*, 99:022503, Jul 2007.
- [3] P. Adrich, A. M. Amthor, D. Bazin, M. D. Bowen, B. A. Brown, C. M. Campbell, J. M. Cook, A. Gade, D. Galaviz, T. Glasmacher, S. McDaniel, D. Miller, A. Obertelli, Y. Shimbara, K. P. Siwek, J. A. Tostevin, and D. Weisshaar. In-beam  $\gamma$ -ray spectroscopy and inclusive two-proton knockout cross section measurements at  $n \approx 40$ . *Phys. Rev. C*, 77:054306, May 2008.
- [4] M. Stanoiu, D. Sohler, O. Sorlin, F. Azaiez, Zs. Dombrádi, B. A. Brown, M. Bellegruic, C. Borcea, C. Bourgeois, Z. Dlouhy, Z. Elekes, Zs. Fülöp, S. Grévy, D. Guillemaud-Mueller, F. Ibrahim, A. Kerek, A. Krasznahorkay, M. Lewitowicz, S. M. Lukyanov, S. Mandal, J. Mrázek, F. Negoita, Yu.-E. Penionzhkevich, Zs. Podolyák, P. Roussel-Chomaz, M. G. Saint-Laurent, H. Savajols, G. Sletten, J. Timár, C. Timis, and A. Yamamoto. Disappearance of the  $n = 14$  shell gap in the carbon isotopic chain. *Phys. Rev. C*, 78:034315, Sep 2008.
- [5] F. Nowacki, A. Poves, E. Caurier, and B. Bounthong. Shape coexistence in  $^{78}\text{Ni}$  as the portal to the fifth island of inversion. *Phys. Rev. Lett.*, 117:272501, Dec 2016.
- [6] J.G. Li. Merging of the island of inversion at  $n = 40$  and  $n = 50$ . *Physics Letters B*, 840:137893, 2023.
- [7] C. R. Hoffman, B. P. Kay, and J. P. Schiffer. Neutron  $s$  states in loosely bound nuclei. *Phys. Rev. C*, 89:061305, Jun 2014.
- [8] S. M. Lenzi, F. Nowacki, A. Poves, and K. Sieja. Island of inversion around  $^{64}\text{Cr}$ . *Phys. Rev. C*, 82:054301, Nov 2010.
- [9] H. L. Crawford, R. M. Clark, P. Fallon, A. O. Macchiavelli, T. Baugher, D. Bazin, C. W. Beausang, J. S. Berryman, D. L. Bleuel, C. M. Campbell, M. Cromaz, G. de Angelis, A. Gade, R. O. Hughes, I. Y. Lee, S. M. Lenzi, F. Nowacki, S. Paschalis, M. Petri, A. Poves, A. Ratkiewicz, T. J. Ross, E. Sahin, D. Weisshaar, K. Wimmer, and R. Winkler. Quadrupole collectivity in neutron-rich fe and cr isotopes. *Phys. Rev. Lett.*, 110:242701, Jun 2013.
- [10] F. Flavigny, D. Pauwels, D. Radulov, I. J. Darby, H. De Witte, J. Diriken, D. V. Fedorov, V. N. Fedosseev, L. M. Fraile, M. Huyse, V. S. Ivanov, U. Köster, B. A. Marsh, T. Otsuka, L. Popescu, R. Raabe, M. D. Seliverstov, N. Shimizu, A. M. Sjödin, Y. Tsunoda, P. Van den Bergh, P. Van Duppen, J. Van de Walle, M. Venhart, W. B. Walters, and K. Wimmer. Characterization of the low-lying  $0^+$  and  $2^+$  states in  $^{68}\text{Ni}$  via  $\beta$  decay of the low-spin  $^{68}\text{Co}$  isomer. *Phys. Rev. C*, 91:034310, Mar 2015.
- [11] B Olaizola, L M Fraile, H Mach, A Poves, A Aprahamian, J A Briz, J Cal-González, D Ghița, U Köster, W Kurcewicz, S R Leshner, D Pauwels, E Picado, D Radulov, G S Simpson, and J M Udías. Beta decay of  $^{66}\text{mn}$  to the  $n= 40$  nucleus  $^{66}\text{fe}$ . *Jour. Phys. G*, 44(12):125103, 2017.

- [12] B.P. Crider, C.J. Prokop, S.N. Liddick, M. Al-Shudifat, A.D. Ayangeakaa, M.P. Carpenter, J.J. Carroll, J. Chen, C.J. Chiara, H.M. David, A.C. Dombos, S. Go, R. Grzywacz, J. Harker, R.V.F. Janssens, N. Larson, T. Lauritsen, R. Lewis, S.J. Quinn, F. Recchia, A. Spyrou, S. Suchyta, W.B. Walters, and S. Zhu. Shape coexistence from lifetime and branching-ratio measurements in  $68,70\text{Ni}$ . *Phys. Lett. B*, 763:108–113, 2016.
- [13] Takaharu Otsuka, Toshio Suzuki, Rintaro Fujimoto, Hubert Grawe, and Yoshinori Akaishi. Evolution of nuclear shells due to the tensor force. *Phys. Rev. Lett.*, 95:232502, Nov 2005.
- [14] B. Olaizola, L. M. Fraile, H. Mach, A. Aprahamian, J. A. Briz, J. Cal-González, D. Ghița, U. Köster, W. Kurcewicz, S. R. Leshner, D. Pauwels, E. Picado, A. Poves, D. Radulov, G. S. Simpson, and J. M. Udías.  $\beta^-$  decay of  $^{65}\text{Mn}$  to  $^{65}\text{Fe}$ . *Phys. Rev. C*, 88:044306, Oct 2013.
- [15] C. Babcock, H. Heylen, J. Billowes, M.L. Bissell, K. Blaum, P. Campbell, B. Cheal, R.F. Garcia Ruiz, C. Geppert, W. Gins, M. Kowalska, K. Kreim, S.M. Lenzi, I.D. Moore, R. Neugart, G. Neyens, W. Nörtershäuser, J. Papuga, and D.T. Yordanov. Evidence for Increased neutron and proton excitations between  $^{51-63}\text{Mn}$ . *Phys. Lett. B*, 750:176, Nov 2015.
- [16] Yusuke Tsunoda, Takaharu Otsuka, Noritaka Shimizu, Michio Honma, and Yutaka Utsuno. Novel shape evolution in exotic Ni isotopes and configuration-dependent shell structure. *Phys. Rev. C*, 89:031301, Mar 2014.
- [17] C. Santamaria, C. Louchart, A. Obertelli, V. Werner, P. Doornenbal, F. Nowacki, G. Authalet, H. Baba, D. Calvet, F. Châteaueau, A. Corsi, A. Delbart, J.-M. Gheller, A. Gillibert, T. Isobe, V. Lapoux, M. Matsushita, S. Momiyama, T. Motobayashi, M. Niikura, H. Otsu, C. Péron, A. Peyaud, E. C. Pollacco, J.-Y. Roussé, H. Sakurai, M. Sasano, Y. Shiga, S. Takeuchi, R. Taniuchi, T. Uesaka, H. Wang, K. Yoneda, F. Browne, L. X. Chung, Zs. Dombradi, S. Franchoo, F. Giacoppo, A. Gottardo, K. Hadynska-Klek, Z. Korkulu, S. Koyama, Y. Kubota, J. Lee, M. Lettmann, R. Lozeva, K. Matsui, T. Miyazaki, S. Nishimura, L. Olivier, S. Ota, Z. Patel, N. Pietralla, E. Sahin, C. Shand, P.-A. Söderström, I. Stefan, D. Steppenbeck, T. Sumikama, D. Suzuki, Zs. Vajta, J. Wu, and Z. Xu. Extension of the  $n = 40$  island of inversion towards  $n = 50$ : Spectroscopy of  $^{66}\text{Cr}$ ,  $^{70,72}\text{Fe}$ . *Phys. Rev. Lett.*, 115:192501, Nov 2015.
- [18] E. Caurier, F. Nowacki, and A. Poves. Merging of the islands of inversion at  $n = 20$  and  $n = 28$ . *Phys. Rev. C*, 90:014302, Jul 2014.
- [19] H. L. Crawford, P. Fallon, A. O. Macchiavelli, R. M. Clark, B. A. Brown, J. A. Tostevin, D. Bazin, N. Aoi, P. Doornenbal, M. Matsushita, H. Scheit, D. Steppenbeck, S. Takeuchi, H. Baba, C. M. Campbell, M. Cromaz, E. Ideguchi, N. Kobayashi, Y. Kondo, G. Lee, I. Y. Lee, J. Lee, K. Li, S. Michimasa, T. Motobayashi, T. Nakamura, S. Ota, S. Paschalis, M. Petri, T. Sako, H. Sakurai, S. Shimoura, M. Takechi,



- Y. Togano, H. Wang, and K. Yoneda. Shell and shape evolution at  $n = 28$ : The  $^{40}\text{Mg}$  ground state. *Phys. Rev. C*, 89:041303, Apr 2014.
- [20] K. Wimmer and P. Doornenbal. Evolution of collectivity and magic numbers in exotic nuclei. *Prog. Part. Nucl. Phys.*, To be published.
- [21] R. Silwal, C. Andreoiu, B. Ashrafkhani, J. Bergmann, T. Brunner, J. Cardona, K. Dietrich, E. Dunling, G. Gwinner, Z. Hockenbery, J.D. Holt, C. Izzo, A. Jacobs, A. Javaji, B. Kootte, Y. Lan, D. Lunney, E.M. Lykiardopoulou, T. Miyagi, M. Mougeot, I. Mukul, T. Murböck, W.S. Porter, M. Reiter, J. Ringuette, J. Dilling, and A.A. Kwiatkowski. Summit of the  $n=40$  island of inversion: Precision mass measurements and ab initio calculations of neutron-rich chromium isotopes. *Phys. Lett. B*, 833:137288, 2022.
- [22] S. M. Lenzi. priv. comm, 2022.
- [23] S. Suchyta, S. N. Liddick, C. J. Chiara, W. B. Walters, M. P. Carpenter, H. L. Crawford, G. F. Grinyer, G. Gürdal, A. Klose, E. A. McCutchan, J. Pereira, and S. Zhu.  $\beta$  and isomeric decay of  $^{64}\text{V}$ . *Phys. Rev. C*, 89:067303, Jun 2014.
- [24] K. Wimmer, F. Recchia, S.M. Lenzi, S. Riccetto, T. Davinson, A. Estrade, C.J. Griffin, S. Nishimura, F. Nowacki, V. Phong, A. Poves, P.-A. Söderström, O. Aktas, M. Al-Aqeel, T. Ando, H. Baba, S. Bae, S. Choi, P. Doornenbal, J. Ha, L. Harkness-Brennan, T. Isobe, P.R. John, D. Kahl, G. Kiss, I. Kojouharov, N. Kurz, M. Labiche, K. Matsui, S. Momiyama, D.R. Napoli, M. Niikura, C. Nita, Y. Saito, H. Sakurai, H. Schaffner, P. Schrock, C. Stahl, T. Sumikama, V. Werner, W. Witt, and P.J. Woods. First spectroscopy of  $^{61}\text{Ti}$  and the transition to the Island of Inversion at  $N = 40$ . *Phys. Lett. B*, 792:16, 2019.
- [25] R. Lică, G. Benzoni, T. R. Rodríguez, M. J. G. Borge, L. M. Fraile, H. Mach, A. I. Morales, M. Madurga, C. O. Sotty, V. Vedia, H. De Witte, J. Benito, R. N. Bernard, T. Berry, A. Bracco, F. Camera, S. Ceruti, V. Charviakova, N. Cieplicka-Oryńczak, C. Costache, F. C. L. Crespi, J. Creswell, G. Fernandez-Martínez, H. Fynbo, P. T. Greenlees, I. Homm, M. Huyse, J. Jolie, V. Karayonchev, U. Köster, J. Konki, T. Kröll, J. Kurcewicz, T. Kurtukian-Nieto, I. Lazarus, M. V. Lund, N. Mărginean, R. Mărginean, C. Mihai, R. E. Mihai, A. Negret, A. Orduz, Z. Patyk, S. Pascu, V. Pucknell, P. Rahkila, E. Rapisarda, J. M. Regis, L. M. Robledo, F. Rotaru, N. Saed-Samii, V. Sánchez-Tembleque, M. Stanoiu, O. Tengblad, M. Thuerauf, A. Turturica, P. Van Duppen, and N. Warr. Evolution of deformation in neutron-rich  $ba$  isotopes up to  $a = 150$ . *Phys. Rev. C*, 97:024305, Feb 2018.
- [26] Kris Heyde and John L. Wood. Shape coexistence in atomic nuclei. *Reviews of Modern Physics*, 83(4):1467, nov 2011.
- [27] J. M. Daugas, I. Matea, J.-P. Delaroche, M. Pfützner, M. Sawicka, F. Becker, G. Bélier, C. R. Bingham, R. Borcea, E. Bouchez, A. Buta, E. Dragulescu, G. Georgiev, J. Giovinazzo, M. Girod, H. Grawe, R. Grzywacz, F. Hammache, F. Ibrahim, M. Lewitowicz, J. Libert, P. Mayet, V. Méot, F. Negoita,

- F. de Oliveira Santos, O. Perru, O. Roig, K. Rykaczewski, M. G. Saint-Laurent, J. E. Sauvestre, O. Sorlin, M. Stanoiu, I. Stefan, Ch. Stodel, Ch. Theisen, D. Verney, and J. Żylicz.  $\beta$ -decay measurements for  $n > 40$  mn nuclei and inference of collectivity for neutron-rich fe isotopes. *Phys. Rev. C*, 83:054312, May 2011.
- [28] W. S. Porter, B. Ashrafkhani, J. Bergmann, C. Brown, T. Brunner, J. D. Cardona, D. Curien, I. Dedes, T. Dickel, J. Dudek, E. Dunling, G. Gwinner, Z. Hockenbery, J. D. Holt, C. Hornung, C. Izzo, A. Jacobs, A. Javaji, B. Kootte, G. Kripkó-Koncz, E. M. Lykiardopoulou, T. Miyagi, I. Mukul, T. Murböck, W. R. Plaß, M. P. Reiter, J. Ringuette, C. Scheidenberger, R. Silwal, C. Walls, H. L. Wang, Y. Wang, J. Yang, J. Dilling, and A. A. Kwiatkowski. Mapping the  $n = 40$  island of inversion: Precision mass measurements of neutron-rich fe isotopes. *Phys. Rev. C*, 105:L041301, Apr 2022.
- [29] A. Gade, R. V. F. Janssens, D. Bazin, P. Farris, A. M. Hill, S. M. Lenzi, J. Li, D. Little, B. Longfellow, F. Nowacki, A. Poves, D. Rhodes, J. A. Tostevin, and D. Weisshaar. In-beam  $\gamma$ -ray spectroscopy of  $^{62,64}\text{Cr}$ . *Phys. Rev. C*, 103:014314, Jan 2021.
- [30] T. Nilsson and O. Tengblad. IS633: Electron capture of 8B into highly excited states in 8Be. <http://cds.cern.ch/record/2222324/files/INTC-P-482.pdf>.
- [31] L. P. Gaffney. I169: Molecular beams of neutron-rich cerium isotopes for coulomb-excitation experiments. <http://cds.cern.ch/record/2157121/files/INTC-I-169.pdf>.

# Appendix

## DESCRIPTION OF THE PROPOSED EXPERIMENT

The experimental setup comprises: (*name the fixed-ISOLDE installations, as well as flexible elements of the experiment*)

Part of the	Availability	Design and manufacturing
(if relevant, name fixed ISOLDE installation: MINIBALL + only CD, MINIBALL + T-REX)	<input checked="" type="checkbox"/> Existing	<input checked="" type="checkbox"/> To be used without any modification
[Part 1 of experiment/ equipment]	<input type="checkbox"/> Existing	<input type="checkbox"/> To be used without any modification <input type="checkbox"/> To be modified
	<input type="checkbox"/> New	<input type="checkbox"/> Standard equipment supplied by a manufacturer <input type="checkbox"/> CERN/collaboration responsible for the design and/or manufacturing
[Part 2 of experiment/ equipment]	<input type="checkbox"/> Existing	<input type="checkbox"/> To be used without any modification <input type="checkbox"/> To be modified
	<input type="checkbox"/> New	<input type="checkbox"/> Standard equipment supplied by a manufacturer <input type="checkbox"/> CERN/collaboration responsible for the design and/or manufacturing
[insert lines if needed]		

HAZARDS GENERATED BY THE EXPERIMENT (if using fixed installation:) Hazards named in the document relevant for the fixed [MINIBALL + only CD, MINIBALL + T-REX] installation.

Additional hazards:

Hazards	[Part 1 of experiment/ equipment]	[Part 2 of experiment/ equipment]	[Part 3 of experiment/ equipment]
<b>Thermodynamic and fluidic</b>			
Pressure	[pressure][Bar], [volume][l]		
Vacuum			
Temperature	[temperature] [K]		
Heat transfer			
Thermal properties of materials			
Cryogenic fluid	[fluid], [pressure][Bar], [volume][l]		
<b>Electrical and electromagnetic</b>			
Electricity	[voltage] [V], [current][A]		

Static electricity			
Magnetic field	[magnetic field] [T]		
Batteries	<input type="checkbox"/>		
Capacitors	<input type="checkbox"/>		
<b>Ionizing radiation</b>			
Target material [material]			
Beam particle type (e, p, ions, etc)			
Beam intensity			
Beam energy			
Cooling liquids	[liquid]		
Gases	[gas]		
Calibration sources:	<input type="checkbox"/>		
• Open source	<input type="checkbox"/>		
• Sealed source	<input type="checkbox"/> [ISO standard]		
• Isotope			
• Activity			
Use of activated material:			
• Description	<input type="checkbox"/>		
• Dose rate on contact and in 10 cm distance	[dose][mSV]		
• Isotope			
• Activity			
<b>Non-ionizing radiation</b>			
Laser			
UV light			
Microwaves (300MHz-30 GHz)			
Radiofrequency (1-300 MHz)			
<b>Chemical</b>			
Toxic	[chemical agent], [quantity]		
Harmful	[chem. agent], [quant.]		
CMR (carcinogens, mutagens and substances toxic to reproduction)	[chem. agent], [quant.]		
Corrosive	[chem. agent], [quant.]		
Irritant	[chem. agent], [quant.]		
Flammable	[chem. agent], [quant.]		
Oxidizing	[chem. agent], [quant.]		
Explosiveness	[chem. agent], [quant.]		
Asphyxiant	[chem. agent], [quant.]		

Dangerous for the environment	[chem. agent], [quant.]		
<b>Mechanical</b>			
Physical impact or mechanical energy (moving parts)	[location]		
Mechanical properties (Sharp, rough, slippery)	[location]		
Vibration	[location]		
Vehicles and Means of Transport	[location]		
<b>Noise</b>			
Frequency	[frequency],[Hz]		
Intensity			
<b>Physical</b>			
Confined spaces	[location]		
High workplaces	[location]		
Access to high workplaces	[location]		
Obstructions in passageways	[location]		
Manual handling	[location]		
Poor ergonomics	[location]		

Hazard identification:

Average electrical power requirements (excluding fixed ISOLDE-installation mentioned above): [make a rough estimate of the total power consumption of the additional equipment used in the experiment]: ... kW